

**Tissue engineering of blood vessels using three-dimensional bioprinting of
endothelial and smooth muscle progenitor cells**

PN-III P1-1.1-PD-2016-1660

Phase I report – 2018

Abstract

3D Bioprinting uses 3D printing techniques for making tissues and organs that mimic the natural tissue architecture. Cells, growth factors and biomaterials are associated in a "bioink" that can be printed using the 3D bioprinter to create structures in which cells grow and differentiate. Amniotic fluid stem cells are easy to obtain, have a high proliferation rate, a normal karyotype, long telomeres, do not form tumours, have immunomodulatory capacity and are multipotent. Using 3D bioprinting, the proposed model was constructed, having a uniform tubular structure, resistant to subsequent histological processes, suggesting good resistance and elasticity. The optimal parameters for printing were: 1.1 to 1.2 bar pressure, 1 mm / sec print speed using a 0.2 mm internal needle, temperature 18°C, ultraviolet polymerization 5 seconds / layer, layers number 10, diameter of construct 2.5 mm. Using these parameters were made vascular constructs with a diameter of 2.46 mm, a wall thickness of 1.4 mm and a height of 2.79 mm. In the optical microscopy using histological staining of the vascular construct sections was observed a network formed by the collagen, hyaluronic acid and polyethylene glycol hydrogel that could permit the attachment of cells and nutrients diffusion. Biological fluids up-take and enzymatic degradation tests that vascular constructs are hydrophilic and biodegradable. Cells isolate from amniotic fluid are mesenchymal stem cells with a fibroblast-like phenotype and an increased expression of the pluripotent markers SSEA-1, SSEA-4, TRA1-60, TRA1-81, and mesenchymal markers CD29, CD49e, CD56, CD73, CD90. Endothelial differentiation was performed within 4 weeks; AFSC altering its fibroblast-like phenotype in an endothelial-like phenotype, ultrastructural characterized by the presence of plasmalemmal endocytosis vesicles. Flow cytometry analysis showed the presence of endothelial cell-specific surface markers, such as CD29, CD31, CD44, CD54, and CD105. In conclusion, collagen and hyaluronic acid hydrogel allow the manufacture of vascular constructs, the parameters of the 3D bioprinter have been optimized so that the vascular model to be similar to the model designed in the BIOCAD software.

Introduction

3D Bioprinting uses 3D printing techniques for manufacture tissues, and organs that mimic the architecture of natural tissues. This technique combines cells, growth factors and biomaterials to create an environment in which cells grow and differentiate into native tissue-like structures. In 3D bioprinting, biomaterials are printed layer by layer to produce structures similar to a desired organ or tissue. The first patent for this technology was proposed in the United States in 2003 and granted in 2006 [1]. Bioprinting involves several steps including: (i) biomaterial selection, (ii) creating a bioprinting pattern using CAM software, (iii) bioprinting using dedicated bioprinters, and (iv) analysing bioprinting constructions. In 3D bioprinting an exhaustive, knowledge and methodology approach is needed using knowledge from various fields such as engineering, tissue engineering, stem cell biology and the science of biomaterials to create an ideal model. An ideal scaffold should be biocompatible, non-immunogenic, non-toxic, anti-thrombotic, with vasoactive properties, and should allow remodelling of the post-implant host tissue. To create such a scaffold, physicochemical parameters such as geometry, surface properties, pore size, adhesion, degradation and biocompatibility should be analysed [2, 3]. Although there is a wide variety of biological materials, including hydrogels, extracellular matrix, fibrillated polymers, microcarrier structures, and cell aggregates, several aspects have to be considered for obtaining structures similar to the target tissue. First of all, an important aspect is *compatibility* with the different types of printing. Extrusion printing is the most flexible method due to the mechanism and larger diameters of printheads. Drop or laser printing is only used for hydrogels. The second aspect is the *bioprintability* of scaffolds. In this case, the bioprinting of hydrogels is superior to other bioinks. The third aspect is *replicability*, the constructs should be as close as possible to the desired tissue. Scaffold degradation, cell interactions and proliferation are important for tissue formation. The fourth aspect is related to the *bioprinting resolution*, which depends on bioprinting type as well as on bioink. Laser bioprinting of hydrogels has a resolution of $5.6 \pm 2.5 \mu\text{m}$, while the drop or extrusion bioprinting between 50-100 μm . The fifth aspect is *accessibility*. Matrigel TM, fibrin and collagen hydrogels are expensive compared to synthetic polymers. In a scaffold, hundreds of millions of cells are needed so that obtaining them could be intensive, costly and time-consuming.

Other aspects involve: scalability, practicality, mechanical and structural integrity, degradability, commercial availability, immunogenicity and applicability. Despite the multitude of biomaterials that appear daily, relatively little research has been devoted to the development of biomaterials for the bioprinting process. Although a large number of hydrogels have great potential for tissue engineering, only a limited number can be used in bioprinting due to the lack of bioprintability and toxicity of degradation products and to the bioprinter parameters that should be optimized for each specific tissue. There are essential improvements in bioinks technology for bioprinting. In the near future there will be a new field such as developing and designing new materials for bioprinting. The main objectives for improving bioprinting are to minimize cell loss, promote cell-cell interactions, increase mechanical properties, and biocompatibility of 3D bioprinting scaffolds. In the future, new biological materials compatible with 3D bioprinting processes will advance research in the field of tissue engineering and regenerative medicine. Amniotic fluid cells are a heterogeneous population of mesenchymal cells of fetal origin of great importance in regenerative medicine. This population is known to have low immunogenicity, so it is less likely to generate an immune response thus having a high therapeutic potential [4, 5]. Phenotypes found in cell culture in amniotic fluid include epithelial-like and fibroblast-like cells [6]. There are also approximately 0.1-0.5% stem cells defined by c-kit expression (CD117 +) on the cell surface. The regenerative potential of amniotic fluid-derived mesenchymal stem cells (AFSC) derives from their ability to differentiate and reduce immunogenicity [7]. AFSC can differentiate into different cell lines, such as endothelial [8], cardiac [9], neural, bone [10]. AFSC can also be reprogrammed without the use of gene transfer technology for induction of pluripotent stem cells [11]. The literature suggests a strong correlation between AFSC and the cardiovascular system. AFSC have demonstrated the ability to form capillary-like networks when grown in hydrogels and there is also evidence of paracrine signalling when AFSC are indirectly co-cultivated with human cardiac cells thereby modulating cardiac regeneration [13].

The project aims is to develop vascular structures using polymeric hydrogels and endothelial and muscle progenitor cells derived from AFSC using 3D bioprinting. Thus, the goal for 2018 was "Obtaining and characterizing endothelial and muscle progenitor cells and vascular model" with the following activities:

1. *Determining optimal 3D printing parameters and creating vascular structure*
2. *Testing resorption rate of vascular structures under conditions that mimic biological fluids*
3. *Morphological and phenotypic characterization of differentiated muscle and endothelial progenitor cells from AFSC*

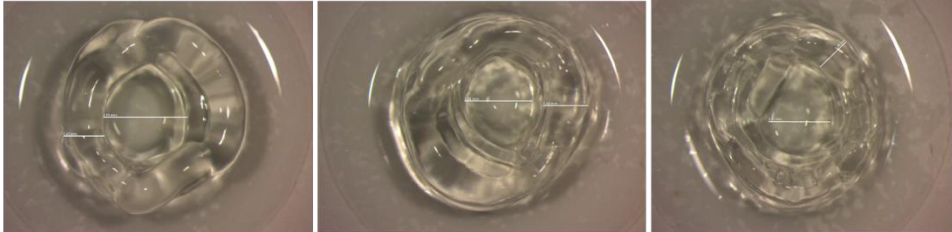
1. Determining optimal 3D printing parameters and creating vascular structure

Establishment of the vascular model was performed using the BIOCAD software. A 10-layer vascular construct having a diameter of 3 mm and a height of 2.5 mm was bioprinted. After each layer, the polymerization module was inserted. A collagen/hyaluronic acid/polyethylene glycol gel was used for printing. The hydrogel polymerization was performed by exposure to UV for 5 seconds / layer. Working pressure has been established according to the physicochemical properties of the printed hydrogel. The optimal pressure is 1.1 - 1.2 bar. Printhead speed is a very important parameter for printing, and is dependent on the physicochemical properties of the hydrogel. At a too high speed it does not close the vascular structure, and at a low speed it creates a thick layer that leads to the formation of a vascular construct over the desired size. The printing speed was set at 1 mm / sec using a needle with 0.2 mm internal diameter. For optimum printing, the hydrogel was printed at 18°C, with the 3D Discovery bioprinter which have the possibility to adjust the printhead temperature (Figure 1).

Diameter of construct	Number of layers	Pressure	UV	Speed rate	Temperature	Needle diameter
2.5 mm	10	1.1 bar	5 seconds	1mm/sec	18°C	0.2 mm

Figure 1. Optimal printing parameters of vascular constructs using collagen / hyaluronic acid / polyethylene glycol hydrogel

Using these parameters, vascular constructs with a diameter of 2.46 mm (\pm 0.41), wall thickness of 1.4 mm (\pm 0.10) and a height of 2.79 mm (\pm 0.05) (Figure 2) were bioprinted. These results show that the hydrogel can be used for vascular constructs and meet the desired requirements for reproduce with accuracy the model created in the BIOCAD.



CONSTRUCT	Diameter	Wall thickness	Height
Construct 1	2,95 mm	1,43 mm	2,73 mm
Construct 2	2,24 mm	1,49 mm	2,82 mm
Construct 3	2,21 mm	1,28 mm	2,84 mm

Figure 2. Measurements of bioprinting vascular constructs after optimization of 3D Discovery bioprinter parameters.

The morphological characterization of vascular constructs was performed by optical microscopy after histological preparation and microtome frozen sections of vascular constructs. The sections were stained by Haematoxylin & Eosin and Trichromic Masson techniques. For the microtome sections, constructs were fixed with PFA 4%, 30 minutes at room temperature, then washed with phosphate buffer and passed through 4%, 5%, 10%, 20% and 50% glycerol baths for cryoprotection. The constructs were covered with OCT and cut to the microtome at a thickness of 5 μ m. The sections were then stained using the classic histological staining techniques.

The results showed that the structures exhibit a tubular, uniform structure, resistant to subsequent histological procedures, which suggests good resistance and elasticity. These latter two aspects will be deepened in stage 2 of the project using rheology and elasticity techniques. Optical microscope imaging of the sections shows a relatively uniform network structure, which would allow the attachment of cells and the exchange of nutrients and gases. By histological staining of the sections, was revealed the network structure of collagen and hyaluronic acid hydrogel (Figure 3).

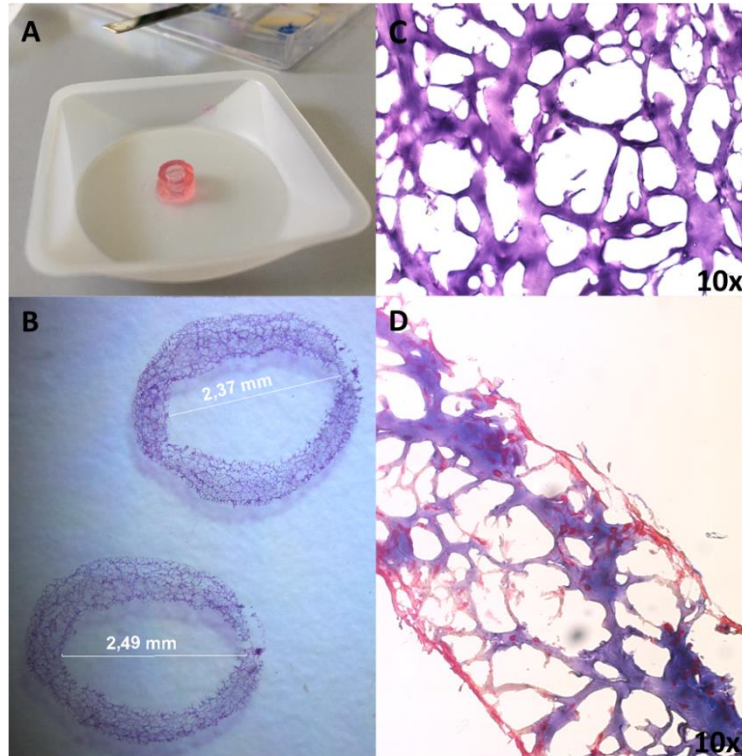


Figure 3. Macroscopic and microscopic morphology of bioprinting vascular constructs. (A) Macroscopic structure of bioprinted vascular construct; (B) Histology sections of vascular constructs; (C) H&E staining and (D) Trichromic Masson of bioprinted of vascular construct sections

2. Resorption rate test of vascular constructs under conditions that mimic biological fluids

Reabsorption experiments were performed to demonstrate the hydrogel behaviour in the presence of water and other fluids. Bioprinting constructs were weighted after printing, then immersed into PBS and weighed at 1, 2, 4, and 24 hours. The resorption rate was calculated according to the formula:

$$\text{Wateruptake} = \frac{W_w - W_d}{W_d(\text{g/g})} \times 100$$

where: W_w = construct weight after immersion in the fluid at time t ; W_d = construct weight before immersion

The results showed that the hydrogel absorbs maximum of PBS at 2 hours after immersion, having a weight gain of 22.32% against the control construct. At 4 and 24 hours the values are similar to those of 1 hour (18%), suggesting that the hydrogel is balanced with the medium within 4 hours (Figure 4).

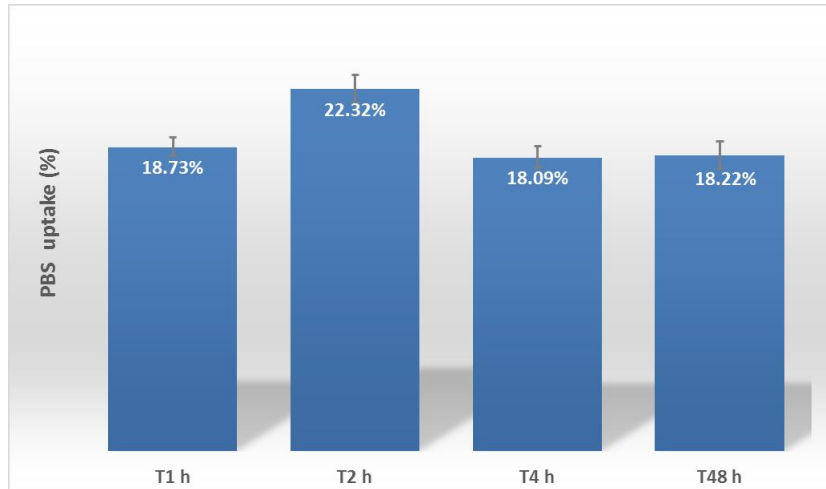


Figure 4. Hydration of biprinted vascular constructs in saline phosphate buffer. Enzymatic degradation of the constructs was revealed using type I collagenase. Biprinted vascular constructs were introduced into culture medium (control constructs) and in collagenase type I medium (10 $\mu\text{g} / \text{ml}$ and 50 $\mu\text{g} / \text{ml}$) and then weighed at different intervals time (30, 60, and 90 minutes). Weight loss was calculated using formula:

$$\% \text{weight loss} = \frac{W_i - W_t}{W_i \times 100}$$

where: W_i = construct weight in collagenase free medium; W_t = construct weight in collagenase type I medium

The results showed a 36.4% and 47% weight loss respectively at 90 minutes after exposure to 10 $\mu\text{g} / \text{ml}$ and 50 $\mu\text{g} / \text{ml}$, collagenase respectively suggesting that the hydrogel is biodegradable (Figure 5).

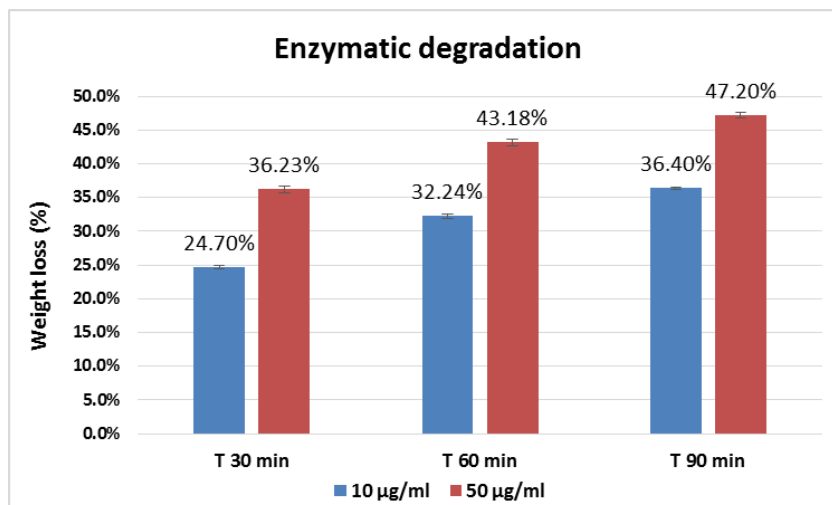


Figure 5. Weight loss of biprinted vascular constructs as a result of enzymatic degradation using type I collagenase

3. Morphological and phenotypic characterization of differentiated muscle and endothelial progenitor cells from AFSC

Amniotic fluid contains several cell types that result from fetal and embryonic tissues, including a population of mesenchymal stem cells. The advantages of these cells are: easy to obtain (used for prenatal diagnosis, and the rest can be used for research or different clinical applications) have a high proliferation rate (population doubling time is ~ 36 hours), can differentiate into adipose, muscle, cardiac, epithelial, neurons, hepatic cells. They have long telomeres, they do not form tumours, they have immunomodulatory capacity and are multipotent. Cells were harvested by centrifugation of the amniotic fluid for 10 minutes at 400g and cultivation of the sediment in BIOAMF-2 culture medium. After 5 days, the medium was changed to remove non-adherent cells, and then the medium changed twice a week. For cell differentiation, they were grown in EGM-2 medium (Endothelial Growth Medium) supplemented with growth factors: VEGF 40 ng / ml; IGF-1 20 ng / ml; EGF 10 ng / ml; β FGF 10 ng / ml; ECGF 10 μ l / ml medium. Cytokines were added every medium changes.

After 4 weeks of growing in endothelial differentiation medium, AFSC changes its morphology from a fibroblast-like phenotype to an endothelial-like phenotype. By electron microscopy, the presence of plasmalemmal vesicles was observed suggesting that they had endocytosis capacity like endothelial cells (Figure 6).

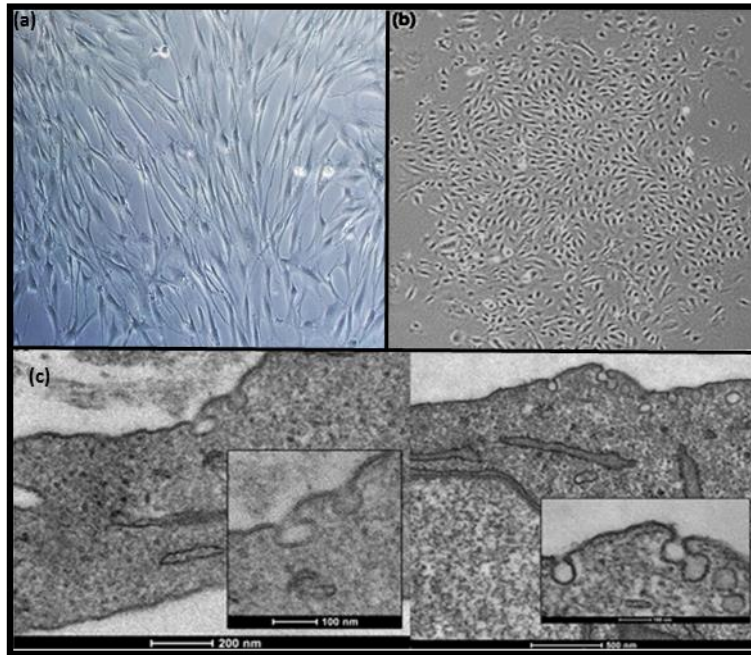


Figure 6. AFSC morphology cultured in BIOAMF medium and in EGM-2 endothelial differentiation medium supplemented with 40 ng / ml VEGF growth factors; IGF-1 20 ng / ml; EGF 10 ng / ml; β FGF 10 ng / ml, ECGF 10 μ l / ml. (a) AFSC cultured in BIOAMF medium presents a fibroblast-like phenotype. (b) AFSC cultivated for 4 weeks in the EGM-2 medium shows an epithelial-like phenotype. (c) The AFSC ultrastructure cultivated in EGM-2 differentiation medium revealed the presence of plasmalemmal vesicles.

AFSC immunophenotype before and after differentiation was assessed by flow cytometry technique. Pluripotent markers (SSEA-1 SSEA-4, TRA1-60, TRA1-81) and markers specific for mesenchymal and endothelial stem cells: CD29, CD31, CD44, CD49e, CD54, CD56, CD73, CD90, CD133 was used for characterisation. AFSC were trypsinized and labelled with PE or FITC-antibodies (100,000 cells / 10 μ l antibody). The cells were incubated 1 hour at room temperature in the dark, then washed with PBS and centrifuged for 10 minutes at 300g to remove unbound antibodies. The cell pellet was mixed in 300 μ l of PBS and analysed on the Gallios flow cytometer (Beckman Coulter).

The results showed that cells isolated from amniotic fluid are stem cells with increased expression of SSEA-1 (72.8%), SSEA-4 (85.3%), TRA1-60 (94.5%) and TRA1-81 (89.2) % (Figure 7).

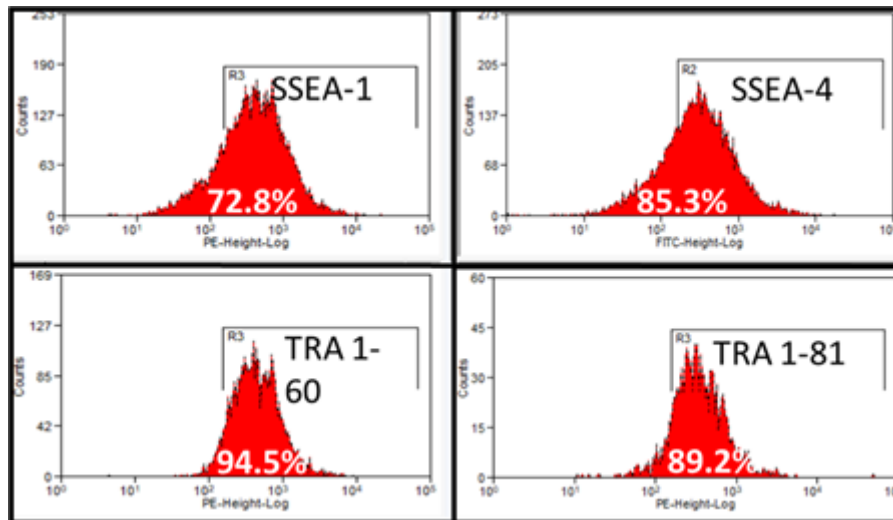


Figure 7. Stem cell-specific pluripotent markers present on the undifferentiated AFSC surface

AFSC cultured in BIOAMF medium exhibits a mesenchymal phenotype characterized by surface markers CD29 (54.8%), CD44 (22.8%), CD49e (99.8%), CD56 (75.2%), CD73 (97.5%), CD90 (98.4%) (Figure 8). CD29 is $\beta 1$ integrin, associates with integrin $\alpha 1$ and $\alpha 2$ forming collagen receptors. It is expressed on the surface of mesenchymal cells and generally on the surface of the adherent cells where it binds the actin cytoskeleton with the extracellular matrix and transmits two-way signals between the extracellular matrix and the cytoplasm. Homing cellular adhesion molecule (HCAM) is a surface glycoprotein involved in cell-cell interactions in cell adhesion and migration. CD44 may also function as a receptor for hyaluronic acid and may interact with other ligands such as osteopontin, collagen and matrix metalloproteinases. CD49e is $\alpha 5$ integrin which in combination with $\beta 1$ integrin forms the fibronectin receptor. CD56 (NCAM) is part of the adhesion molecule family being neuronal cells. Data from the literature and previous results have shown that AFSC have an increased potential for differentiation in neural cells, so the medium in which they are cultivated and the duration of cell cultures is very important [13]. CD73 and CD90 are markers specific to mesenchymal adherent cells.

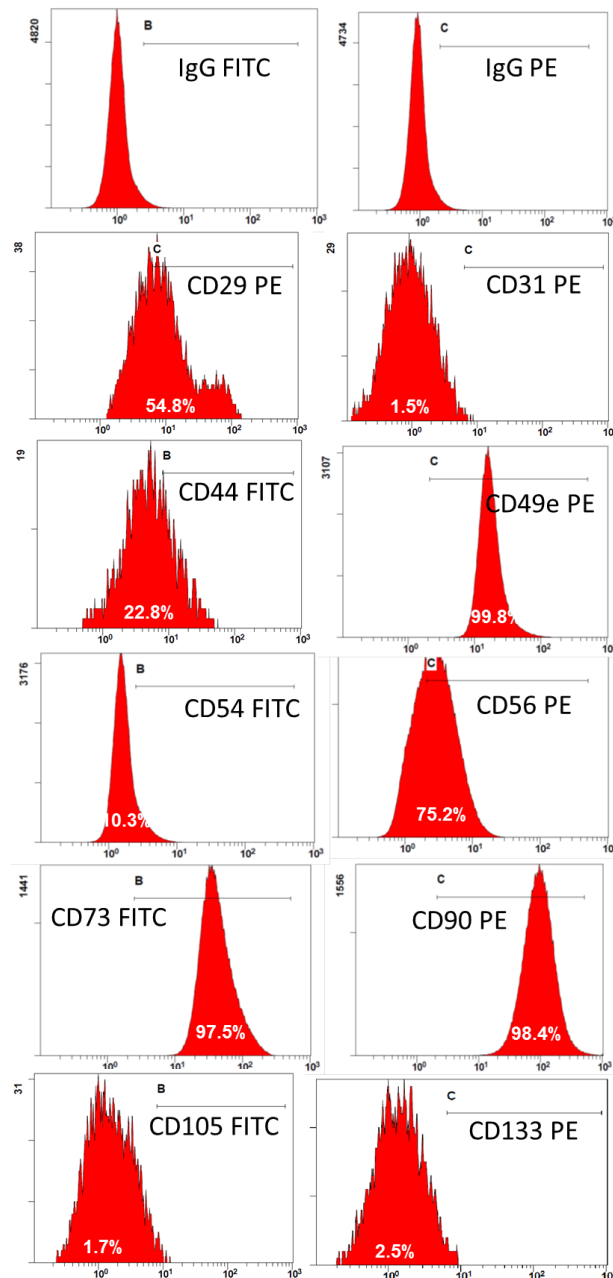


Figure 8. Immunophenotype profile of AFSC cultivated in BIOAMF medium

After growing AFSC in EGM-2 medium supplemented with 40 ng / ml VEGF growth factors, 20 ng / ml IGF-1, 10 ng / ml EGF, 10 ng / ml β FGF and 10 μ l / ml ECGF for 4 weeks flow cytometry assay showed the presence of endothelial cell-specific surface markers. Expression of CD29 (98.4%) increased in EGM-2, and CD56 (12%) decreased, suggesting that cells switched neuronal differentiation to an endothelial phenotype. Endothelial cell markers present on the surface of cells were: CD31 (50.7%), CD54 (58.3%), CD105 (67.2%) (Figure 9). CD31 (platelet endothelial cell adhesion molecule) is a platelet and endothelial cell specific adhesion molecule

involved in angiogenesis, vasculogenesis, integrin activation and leukocyte migration. Intercellular adhesion molecule 1 (ICAM-1) is an immunoglobulin family glycoprotein mediated on the surface of immune and endothelial cells, facilitating transmigration of leukocytes through vascular endothelium. CD105 (endoglin) is a protein involved in angiogenesis being found on the surface of vascular and endothelial progenitor cells.

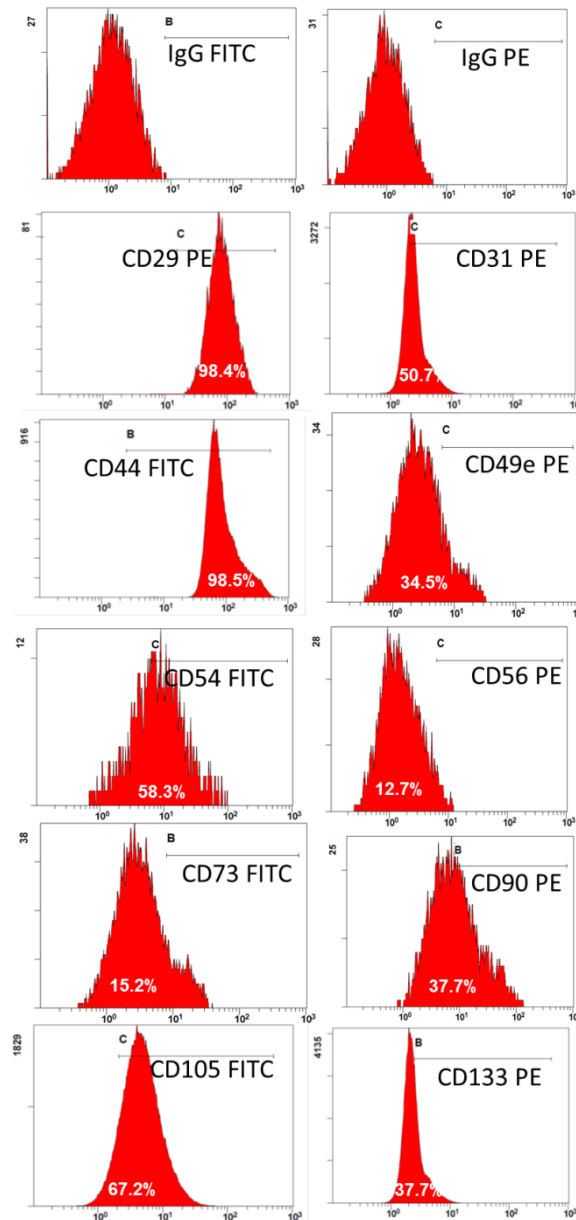


Figure 9. Immunophenotype profile of AFSC cultivated in the endothelial differentiation medium EGM-2

In conclusion, the collagen/hyaluronic acid hydrogel allows the creation of the vascular constructs; the parameters of the 3D bioprinter have been optimized so that a vascular structure similar to the model developed in the BIOCAD program can be created. Amniotic fluid isolated cells are mesenchymal stem cells with potential for differentiation to other cell lines. Following the project, the cells will be differentiated into endothelial and muscle cells and then incorporated into the hydrogel and bioprinting of the vascular structure. Furthermore the bioprinted constructs will be characterized regarding biocompatibility and interactions between cells.

References

1. Thomas J.D. Could 3D bioprinted tissues offer future hope for microtia treatment. *International Journal of Surgery*, 32, 43-44, 2016
2. Chua C.K., Yeong W.Y. *Bioprinting: Principles and Applications*. Singapore: World Scientific Publishing Co., 2015.
3. Datta P, Ayan B, Ozbolat IT. Bioprinting for vascular and vascularized tissue biofabrication. *Acta Biomaterialia* 51, 1–20, 2017.
4. Abdulrazzak H, De Coppi P, Guillot PV. Therapeutic potential of amniotic fluid stem cells. *Curr Stem Cell Res Ther*. 8(2):117-24, 2013.
5. Pozzobon M, Piccoli M, Schiavo AA, Atala A, De Coppi P. Isolation of c-Kit+ human amniotic fluid stem cells from second trimester. *Methods Mol Biol*. 1035:191-8, 2013.
6. Pipino C, Pierdomenico L, Di Tomo P, Di Giuseppe F, Cianci E, D'Alimonte I, Morabito C, Centurione L, Antonucci I, Marigliò MA, Di Pietro R, Ciccarelli R, Marchisio M, Romano M, Angelucci S, Pandolfi A. Molecular and phenotypic characterization of human amniotic fluid-derived cells: a morphological and proteomic approach. *Stem Cells Dev*. 24(12):1415-28, 2015.
7. Cananzi M, De Coppi P. CD117+ amniotic fluid stem cells: State of the art and future perspectives. *Organogenesis* 8:3, 77-88, 2012.
8. Benavides OM, Quinn JP, Pok S, Petsche Connell J, Ruano R, Jacot JG. Capillary-Like Network Formation by Human Amniotic Fluid-Derived Stem Cells Within Fibrin/Poly(Ethylene Glycol) Hydrogels. *Tissue Eng Part A*. 21(7-8):1185-94, 2014.
9. Connell JP, Ruano R, Jacot JG. Amniotic fluid-derived stem cells demonstrate limited cardiac differentiation following small molecule-based modulation of Wnt signaling pathway. *Biomed Mater*. 10(3):034103, 2015.

10. Resca E, Zavatti M, Maraldi T, Bertoni L, Beretti F, Guida M, La Sala GB, Guillot PV, David AL, Sebire NJ, De Pol A, De Coppi P. Enrichment in c-Kit improved differentiation potential of amniotic membrane progenitor/stem cells. *Placenta*. 36(1):18-26, 2015.
11. Spinelli V, Guillot V.P., De Coppi P. Induced pluripotent stem (iPS) cells from human fetal stem cells (hFSCs). *Organogenesis*, 9(2):101–110, 2013.
12. Mirabella T, Hartinger J, Lorandi C, Gentili C, van Griensven M, Cancedda R. Proangiogenic soluble factors from amniotic fluid stem cells mediate the recruitment of endothelial progenitors in a model of ischemic fasciocutaneous flap. *Stem Cells Dev.*, 21(12):2179-2188, 2012.
13. Iordache F, Constantinescu A, Andrei E, Amuzescu B, Halitzchi F, Savu L, Maniu H. Electrophysiology, immunophenotype, and gene expression characterization of senescent and cryopreserved human amniotic fluid stem cells. *J Physiol Sci.*, 66(6):463-476, 2016

27.11.2018

Project Director,
Dr. Florin Iordache